Fiber Bragg grating modeling, simulation and characteristics with different grating lengths

Ho Sze Phing*, Jalil Ali, Rosly Abdul Rahman and Bashir Ahmed Tahir

Advanded Optics and Photonics Technology Center, Department of Physics, Faculty of Science, Universiti Teknologi Malaysia, 81310 UTM Skudai, Johor, Malaysia
*To whom correspondence should be addressed. E-mail: hoszephing@gmail.com

ABSTRACT

In this paper we perform a simulation of fiber Bragg grating sensor with different grating lengths. It is shown that the grating length represents as one of the critical parameters in contributing to a high performance fiber Bragg grating sensor. The simulated fiber gratings with different lengths were analyzed and designed by calculating reflection and transmission spectra, and the bandwidth. Such simulations are based on solving coupled mode equations that describe the interaction of guided modes. The coupled mode equations are solved by the Transfer Matrix Method (a fundamental matrix method).

| Fibre Bragg grating | Simulation | Bandwitdth | Reflectivity | Coupled mode theory | Transfer Matrix Method |

1. Introduction

Intensive research and development efforts to engineer a new class of fiber optic component—the UV-inscribed fiber gratings has been witnessed in the past decade [1], due to its numerous present and future applications in diverse modern optoelectronics, optical fiber sensor and optical fiber communication systems [2].

The concept of fiber Bragg gratings has been around for some time and was first reported in 1978 by Hill [3]. However, the much recognized pioneering work at the United Technology Research Centre was only published 11 years later [4].

FBGs are based on the principle of Bragg reflection. When light propagates by periodically alternating regions of higher and lower refractive index, it is partially reflected at each interface between those regions. If the spacing between those regions is such that all the partial reflections add up in phase—when the round trip of the light between the two reflections is an integral number of wavelengths— the total reflection can grow to nearly 100%, even if the individual reflections are very small. Of course, that condition will only hold for specific wavelengths. For all other wavelengths, the out-of-phase reflections end up cancelling each other, resulting in high transmission.

2. Structure Modeling

Our FBG model, assumes that the power of the UV laser source and the printing exposure time are unlimited. On the other hand, the index variation caused by defect center's bond breaking through the UV light absorption can only be slightly modified because the doping concentration is always limited. This means that the refractive index cannot always respond linearly to the printing conditions (such as UV source power or exposure time). We assume that the grating is uniform along the direction. The index inside the core after the FBG has been printed can be expressed by

$$n(z) = n_{co} + \Delta n_o n_d(z) \tag{2.1}$$

where n_{co} is the refractive index inside the fiber core, Δn_o is the maximum index variation, and $n_d(z)$ can be called the index variation function [2].

3. Theory

Coupled Mode Theory is a method to analyze the light propagation in perturbed or weakly coupled waveguides. The basic idea of the Coupled Mode Theory method is that the modes of the unperturbed or uncoupled structures are defined and solved first. Then, a linear combination of these modes is used as a trial solution to Maxwell's equations for complicated perturbed or coupled structures. After that, the derived coupled mode equations can be solved analytically or by numerical methods. The theory assumes that the field of the coupled structures may be sufficiently represented by a linear superposition of the modes of the unperturbed structures. In many practical cases, this assumption is valid and does give an insightful and often accurate mathematical description of electromagnetic wave propagation.

Assuming the electric field is a linear combination of the ideal modes (with no grating perturbation), such that

$$\vec{E}(z) = \sum_i \left[a_i^{(+)} \exp(-j\beta_i z) + a_i^{(-)} \exp(j\beta_i z) \right] \vec{e}_i \tag{3.1}$$

where $a_i^{(+)}$ and $a_i^{(-)}$ are the slowly varying amplitudes of ith mode traveling in the $+z$ and $-z$ directions. β_i and $\vec{e}_i$ is the propagation constant and modal field of the ith mode. The above electric field is used as a trial solution in the Maxwell's equation [5]. The following Coupled mode Equations (CMEs) can be derived by using the properties of waveguide modes,

$$\frac{da_i^{(+)}}{dz} = -j \cdot \sum_k \{ a_k^{(+)} k_{ki} \exp[-j \cdot (\beta_k - \beta_i) \cdot z] + a_k^{(-)} k_{ki} \exp[j \cdot (\beta_k + \beta_i) \cdot z] \} \tag{3.2}$$

$$\frac{da_i^{(-)}}{dz} = j \cdot \sum_k \{ a_k^{(+)} k_{ki} \exp[-j \cdot (\beta_k + \beta_i) \cdot z] + a_k^{(-)} k_{ki} \exp[j \cdot (\beta_k - \beta_i) \cdot z] \} \tag{3.3}$$

The coupling coefficient between modes k and i is given by:

$$k_{ki} = \frac{1}{4} \omega \varepsilon_0 \iint \tilde{n}^2(x, y, z) \vec{e}_k \cdot \vec{e}_i^* \, dx dy \tag{3.4}$$

$$\widetilde{n}^2(x,y,z) = n^2(x,y,z) - n_0^2(x,y) \tag{3.5}$$

where $\widetilde{n}^2(x,y,z)$ is the periodic refractive index perturbation of the grating, and $n_0(x,y)$ is the index profile of waveguide. $n(x,y,z)$ is the grating index profile.

In our simulation, the coupled mode equations are based on non-orthogonal coupled mode theory. Both the waveguide nature coupling and grating coupling are considered. In order to formulate the coupled mode equations, waveguide modal constants, fields, and coupling coefficients are calculated based on waveguide and grating profiles.

In our work the well-known transfer matrix method is applied to solve the couple mode equations and to obtain the spectral response of the fiber grating. In this approach, the grating is divided into uniform sections, each section is represented by a 2*x*2 matrix. By multiplying these matrices, a global matrix that describes the whole grating is obtained. We will describe the approach developed by Yamada *et al.* [6].

We assume that the refractive index, inside an *i*th uniform section from a Bragg grating, can be described by

$$n(z) = n_{eff} + \Delta n_i \cos(2\pi z / \Lambda_i) \tag{3.6}$$

where n_{eff} is the effective index of fiber core, Δn_i is the refractive index amplitude modulation, and Λ_i is the section grating period.

A non-uniform fiber grating of length *L* is divided into *M* uniform gratings, i. e. section, as illustrated in **Fig. 1**. The propagation through each uniform section *i* is described by a matrix *Fi* defined such that

$$\begin{bmatrix} R_i \\ S_i \end{bmatrix} = F_i \begin{bmatrix} R_{i-1} \\ S_{i-1} \end{bmatrix} \tag{3.7}$$

The matrix F_i for one section is defined by

$$F_i = \begin{bmatrix} \cosh(\gamma_i \Delta z_i) - j\dfrac{\hat{\sigma}_i}{\gamma_i}\sinh(\gamma_i \Delta z_i) & -j\dfrac{\kappa_i}{\gamma_i}\sin g(\gamma_i \Delta z_i) \\[2ex] j\dfrac{\kappa_i}{\gamma_i \sin g(\gamma_i \Delta z_i)} & \cosh(\gamma_i \Delta z_i) + j\dfrac{\hat{\sigma}_i}{\gamma_i}\sinh(\gamma_i \Delta z_i) \end{bmatrix} \tag{3.8}$$

Here $j = \sqrt{-1}$ and S_i are the slowly varying amplitudes of the fundamental mode traveling in the +*z* and –*z* directions, respectively. γ_i is the coupling coefficient defined as $\gamma_i = \sqrt{\kappa_i^2 - \hat{\sigma}_i^2}$, where $\hat{\sigma}_i = \pi\left(\dfrac{2n_{eff}}{\lambda} - \dfrac{1}{N}\right)$, $\kappa_i = \dfrac{\pi}{\lambda}\Delta n_i$, and λ is the wavelength, and Δz_i is the section thickness.
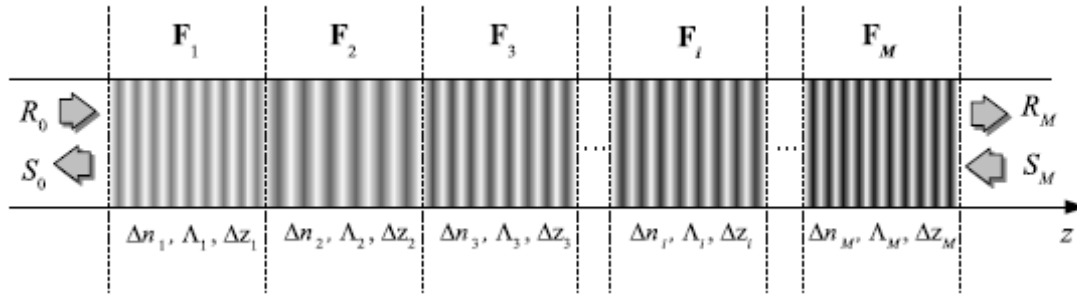
Fig. 1. The transfer matrix method applied to obtain the spectral characteristics of a fiber grating.

Once all the matrices for the individual sections are known, we find the output amplitudes from

$$\begin{bmatrix} R_M \\ S_M \end{bmatrix} = F \begin{bmatrix} R_0 \\ S_0 \end{bmatrix} \quad ; \quad F = F_M \cdot F_{M-1} \cdot ... \cdot F_i \cdot ... \cdot F_1 \cdot \tag{3.9}$$

The reflection coefficient of the entire grating is defined as $\rho = S_0/R_0$ and the reflectivity as $\Gamma = |\rho|^2$ [7, 8]. The main drawback of this method is that M may not be made arbitrarily large, since the coupled-mode theory approximations are not valid when uniform grating section is only a few grating periods long [6]. Thus, it requires $\Delta z \gg \Lambda$.

4.   Simulation Results

We performed our simulations using a set of FBG parameters as below.

Parameters	Settings
Grating shape profile	Sine ; $f(z) = \sin\left(\dfrac{2\pi}{\Lambda} z\right)$
Average index	Uniform
Apodization	User defined
Taper's parameter	w = 0.7 exp (- (2*(x-Length/2) / (Length*w)) ^ 4)
Index modulation	0.0017
Central wavelength	1550 nm
Refractive index of fiber core	1.46
Refractive index of cladding	1.45
Grating period	$\approx 0.534 \ \mu m$

The reason for picking the condition is that this value can make a maximum performance in reflection spectra for a grating length at 10 mm.

It is important to investigate the signal characteristics of FBG sensors because the demodulation method of FBG sensors is based on detecting the wavelength shift of a sensor peak. Among many signal characteristics, a broadening of bandwidth reduces WDM (wavelength division multiplexing) performance and a decrease of reflectivity reduces SNR (signal to noise ratio) for peak detection [9]. There are several definitions of bandwidth. However, the most easily identifiable one is bandwidth between the first minima on either side of the main reflection peak [8]. Bandwidth is a measure of the reflected signals spectral width. It is usually measured at Full Width Half Max (FWHM). Reflectivity is the percentage of light reflected at the Bragg Wavelength. The wavelengths outside of the reflected bandwidth are transmitted without disturbance [10].

4.1   Bandwidth

To examine the bandwidth change of the FBG sensors, FWHM (full width half maximum) values of FBG sensors with five grating lengths, 20, 10, 5, 2 and 1 mm, were measured. Examination of the FWHM of FBG sensor signals is commonly used for elucidating the change of bandwidth. The FWHM denotes the bandwidth with 50% reflectivity (3-dB bandwidth) of a sensor peak. **Fig. 2** shows the change of 3-dB bandwidth of the FBG sensors as the grating length increases. In the case of a 1 mm FBG sensor, the 3-dB bandwidth is 1.4 nm. The bandwidth reduces to 1.08 nm for the grating length of 2 mm. And then, the bandwidth reduced again to 1.04 nm as the grating length increased to 5 mm. The bandwidth did not change after the grating length of 5 mm and is maintained at 1.04 nm for 10 mm and 20 mm. The 3-dB bandwidth showed an exponential decrease over the elevation of grating lengths, and when the grating length was 5 mm, the 3-dB bandwidth is 1.04 nm and maintained subsequently for longer length, as shown in **Fig. 3**. From the above results, upon consideration of the reduction of the FBG sensor signals, it was confirmed that the FBG sensor simulated using parameters defined showed its achievement in stability for a fix bandwidth when the grating length is 5 mm.
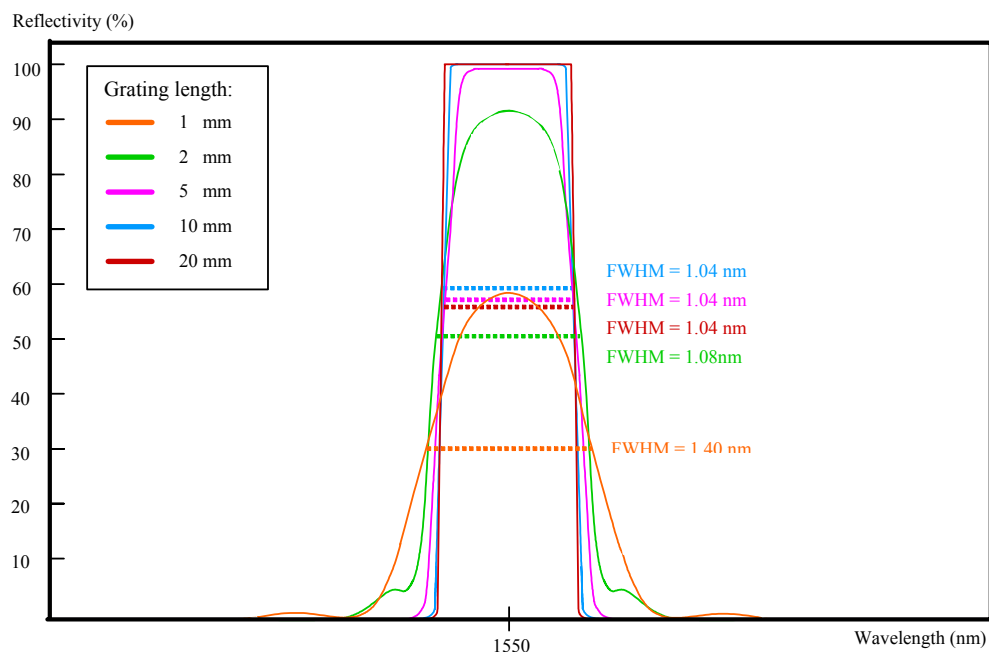
Fig. 2. The bandwidth change of fiber grating sensor as the grating change increases.
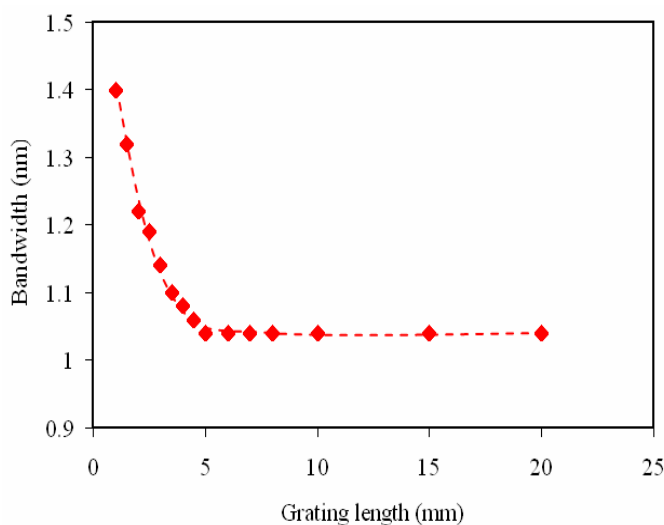
Grating length (mm)	Bandwidth (nm)
1.0	1.40
1.5	1.32
2.0	1.22
2.5	1.19
3.0	1.14
3.5	1.10
4.0	1.08
4.5	1.06
5.0	1.04
6.0	1.04
7.0	1.04
8.0	1.04
10.0	1.04
15.0	1.04
20.0	1.04

**Fig. 3.** The relationship between fiber grating sensor bandwidth and grating lengths.

4.2 Reflectivity/Transmittivity Change

The reflectivity and transmittivity as well as the bandwidth of FBG sensors also changes if they are under different grating lengths. **Fig. 4** indicates the reflectivity and transmittivity change of the FBG sensors with an increase of grating lengths. As shown in **Fig. 4**, the reflectivity increases with the elevation of gratings length. The fiber grating sensor achieved 100% reflection when the grating length is 10 mm and maintained this value for the longer length. This tendency is very similar with the results of 3-dB bandwidth change but in an inverse direction where the reflectivity showed an exponential increase over the elevation of grating lengths, as shown in **Fig. 5**. From the above results, upon consideration of the reflectivity elevation of the FBG sensor signals, it was confirmed that the simulated FBG sensors showed better performance as the grating length increased and achieved 100 % reflection at the grating length of 10 mm.
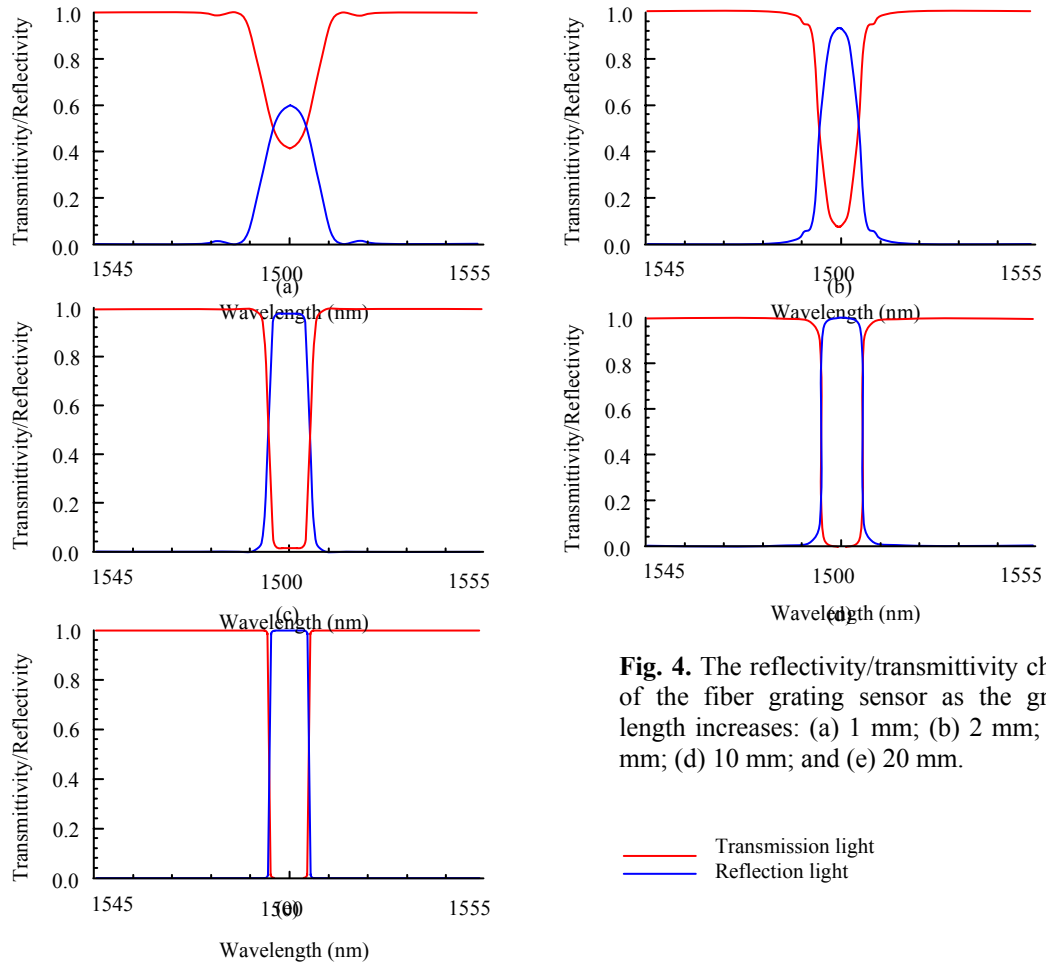
Fig. 4. The reflectivity/transmittivity change of the fiber grating sensor as the grating length increases: (a) 1 mm; (b) 2 mm; (c) 5 mm; (d) 10 mm; and (e) 20 mm.
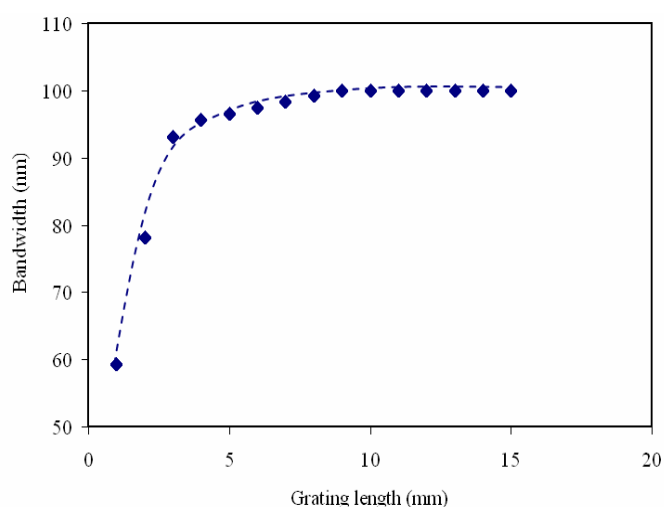
Grating length (mm)	Reflectivity (%)
1.0	59.35
1.5	78.20
2.0	93.13
2.5	95.60
3.0	96.52
3.5	97.41
4.0	98.34
4.5	99.21
5.0	99.97
6.0	99.98
7.0	99.99
8.0	99.99
10.0	100
15.0	100
20.0	100

Fig. 5. The relationship between fiber grating sensor bandwidth and grating lengths.

5. Conclusion

This study investigated the signal characteristics of FBG sensors with various grating lengths using simulation method. We conducted quantitative analyses on the bandwidth reduction and reflectivity elevation with the increases of grating length. The conclusions obtained from this study are as follows.
1. The bandwidth of fiber grating sensor reduces with the increase in grating length.
2. As the grating length increased to 5 mm, the bandwidth of the FBG sensor reduced to 1.04 nm and maintained this value for longer grating length.
3. The reflectivity of fiber grating sensor increases with the increase in grating length.
4. The reflectivity increased with the elevation of grating length in which it achieves 100% in reflection at grating length 10 mm and maintained this value for longer length.

6. Acknowledgement

7. References

[1] L. Zhang, W. Zhang, and I. Bennion, "In-Fiber Grating Optic Sensors", England: Aston University, (2002) 1.
[2] Y. Zhao and J. C. Palais, "Fiber Bragg Grating Coherence Spectrum Modeling, Simulation, and Characteristics", Journal of Lightwave Technology, 15 (1997) 1,
[3] K. O. Hill, B. Malo, F. Bilodeau, D. C. Johnson and J. Albert, "Photosensitivity on optical fiber waveguides: application to reflection filter fabrication", Appl. Phys Lett 32 **(**1978) 747-749.
[4] G. Meltz, W. W. Morey and W. H. Glenn, "Formation of Bragg gratings in optical fiber by a traverse holographic method", Opt. Lett. 14 (1989) 823-825.

[5]   J. C. C. Carvalho, M. J. Sousa, C. S Sales. J´unior, J. C. W. A. Costa, C. R. L. Francˆes and M. E. V. Segatto, "A new acceleration technique for the design of fibre gratings", Optical Society of America, 14(2006) 2.

[6]   M. Yamada and K. Sakuda. "Analysis of almost-periodic distributed feedback slab waveguides via a fundamental matrix approach". Appl. Opt., 26 (1987) 3473–3478.

[7]   T. Erdogan, "Fiber grating spectra", IEEE J. Lightwave Technol., 15 (1997) 1277–1294.

[8]   R. Kashyap, "Fibre Bragg Gratings", Academic Press, San Diego, (1999).

[9]   D.H. Kanga, S.O. Parkb, C.S. Hongb, C.G. Kimb, "The signal characteristics of reflected spectra of fiber Bragg grating sensors with strain gradients and grating lengths", NDT & E International 38 (2005) 712–718.

[10] "Fiber Bragg Gratings", USA: Furukawa Electric North America, Inc., Lightwave Inc., (2005).